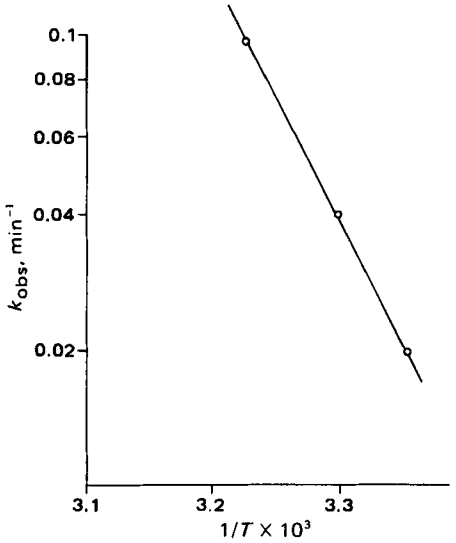

Figure 5—*Arrhenius plot for the hydrolysis of the prodrug at pH 5.6.*

Buffer concentrations of up to 1 *M* acetate buffer at pH 5.4 did not affect the hydrolysis rate.

DISCUSSION

The hydrolysis of the prodrug to aspirin followed first-order kinetics. The most likely mechanism occurring in the pH 3–9 range is an uncatalyzed unimolecular decomposition. The absence of buffer catalysis and the slightly positive entropy of activation make catalysis by water unlikely (10). Additionally, the pronounced effect of the solvent dielectric constant on the hydrolysis rate provides evidence for increasing separation of changes in the transition state. Finally, the absence of a significant solvent deuterium isotope effect provides evidence that specific acid catalysis is not occurring at this pH range.

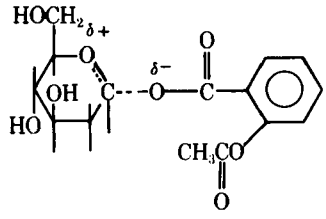

II

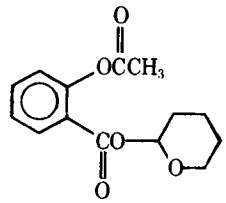

III

Based on these data, it is possible that I hydrolysis proceeds *via* the formation of the charged intermediate (II), which then undergoes simple CO bond cleavage, generating aspirin. In the same pH range, the hydrolysis rate of the corresponding pyran derivative (III) proceeds by a factor of 60 times faster than prodrug I[1].

The data presented show that the transient blocking of the acidic carboxylic group of aspirin by formation of deoxyglucose acylal-linked derivatives can result in a prodrug that regenerates aspirin at an acceptable rate independent of pH. Such a compound could potentially reduce the GI liability of aspirin by presenting a neutral molecule to the gastric membrane. Plans are underway to test this concept *in vivo*.

REFERENCES

(1) J. P. Leonards and G. Levy, *J. Pharm. Sci.*, **59**, 1511 (1970).

(2) K. W. Anderson, *Arch. Int. Pharmacodyn. Ther.*, **152**, 379 (1964).

(3) C. Davison, D. H. Hertig, and R. DeVine, *Clin. Pharmacol. Ther.*, **7**, 329 (1966).

(4) T. S. Pierre and W. P. Jencks, *J. Am. Chem. Soc.*, **90**, 3817 (1968).

(5) G. Levy and B. A. Gagliardi, *J. Pharm. Sci.*, **52**, 730 (1963).

(6) A. DeWeck, *Int. Arch. Allergy*, **41**, 393 (1971).

(7) A. Hussain, M. Yamasaki, and J. E. Truelove, *J. Pharm. Sci.*, **63**, 627 (1974).

(8) G. Akerlof and O. Short, *J. Am. Chem. Soc.*, **58**, 1241 (1936).

(9) R. G. Bates, "Determination of pH Theory and Practice," Wiley, New York, N.Y., 1967.

(10) A. Brown and T. C. Bruice, *J. Am. Chem. Soc.*, **95**, 1593 (1973).

Kinetics and Mechanism of Reaction of *m*-Nitrobenzhydrazide and Other Hydrazines with Acetic Acid

THOMAS MEDWICK ˣ **and HAMED M. ABDOU** *

Received June 20, 1977, from the *College of Pharmacy, Rutgers—the State University of New Jersey, New Brunswick, NJ 08903.* Accepted for publication August 31, 1978. * Present address: E. R. Squibb & Sons, New Brunswick, NJ 08903.

Abstract □ A comprehensive kinetic study was conducted of the reactions of *m*-nitrobenzhydrazide and some other hydrazines with acetic acid. The overall reaction rate for all of the compounds studied followed pseudo-first-order kinetics. The temperature dependence of the *m*-nitrobenzhydrazide degradation reaction was determined. The reaction rate dependence on the acetic acid concentration was found to be close to first order. High-pressure liquid chromatography was used extensively in identifying and measuring the appearance or disappearance rates of *m*-nitrobenzhydrazide degradation products in acetous solution. With *m*-nitrobenzhydrazide, the major degradation products were *N,N'*-bis(*m*-nitrobenzoyl)hydrazine, *N*-acetyl-*N'*-*m*-nitrobenzoylhydrazine, diacetylhydrazine, and hydrazine. The concentration profiles of these products in solution suggested a complex mechanism by which hydrazides react with acetic acid. All eight rate constants at 61° in the suggested mechanism were calculated by an approximation method based on experimental data. The findings in the present study indicate that acetic acid is to be avoided as a solvent for hydrazine derivatives.

Keyphrases □ *m*-Nitrobenzhydrazide—kinetics and mechanism of reaction with acetic acid □ Hydrazine derivatives—kinetics and mechanism of reaction with acetic acid □ Kinetics—reactions of hydrazines with acetic acid

Hydrazides and other hydrazine derivatives constitute a large and important class of organic compounds and have long been used in the chemical and pharmaceutical fields. In analytical chemistry, they are used as good quantitative carbonyl reagents. Although hydrazides are weaker bases than other hydrazine derivatives and, therefore, possess

0022-3549/79/0300-0301$01.00/0

less carbonyl affinity, they are still preferred as carbonyl reagents because of their stability when present as a free base.

In many cases, these reactions of hydrazides with carbonyls were carried out in an acetic acid medium (1–3) because of its enhancement of their basicity. In some instances, assays of hydrazides and other hydrazine derivatives were also performed in acetic acid (4, 5). A serious limitation of this solvent system, however, is the tendency of these compounds to lose their basicity and to degrade rapidly in acetous solution. This degradation process was reported earlier (2, 3, 6), but its mechanism and the degradation products involved have not been studied. In recent work (7) in these laboratories, the reaction kinetics of hydrazine (I) and monoacetylhydrazine (II) with acetic acid were found to behave according to a complex mechanism in which diacetylhydrazine (III) was the main degradation product.

In the present study, the reaction kinetics of some other hydrazines and hydrazides with acetic acid were thoroughly investigated to establish a general mechanism by which most of these compounds degrade. The disappearance rate of a group of compounds in acetous solution was determined by potentiometric titration. However, potentiometric titrations are limited because of their inability to measure the quantities of each degradation product. Thus, potentiometry was used together with TLC and high-pressure liquid chromatography (HPLC) to study a representative compound, *m*-nitrobenzhydrazide (IV).

The degradation of IV was studied in solutions of different acetic acid concentrations in chloroform to establish the rate order with respect to acetic acid. The temperature dependence of the reaction was established. The degradation products were identified, and their disappearance or appearance rates were measured using HPLC. On this basis, a complex kinetic mechanism is suggested to account for the various rates. Approximation methods were used to calculate all rate constants.

EXPERIMENTAL

Reagents, Chemicals, and Solutions—All chemicals were reagent grade unless otherwise specified.

Benzenesulfonylhydrazine[1], 4-phenyl-3-thiosemicarbazide[2], *p*-nitrophenylhydrazine[2], and *p*-bromophenylhydrazine[2] were used as received. Phenylhydrazine[2] was distilled under reduced pressure and nitrogen prior to use.

Semicarbazide (mp 91–95°) was formed by reacting the hydrochloride[2] with sulfuric acid, removing the water under reduced pressure, and reacting the resultant, dried sulfate salt with anhydrous liquid ammonia. The formed ammonium sulfate precipitated and was filtered off; the filtrate was allowed to stand in the hood so that the ammonia would evaporate. The crude semicarbazide was recrystallized from absolute ethanol.

4-Phenylsemicarbazide[1] (mp 124–126°), *m*-nitrobenzhydrazide[2] (mp 153–155°), and *p*-nitrobenzhydrazide[2] (mp 210°) were recrystallized from water.

o-Nitrobenzhydrazide (mp 117–120°) was prepared by refluxing ethyl *o*-nitrobenzoate[1] with hydrazine[2] (97+%, anhydrous) in ethanol for 3 hr (ester to hydrazine molar ratio of 1:2). On cooling the solution, the hydrazide separated and was filtered off. The crude product was recrystallized from water.

Benzhydrazide (mp 110–112°) and *p*-bromobenzhydrazide (mp 165–166°) were prepared using ethyl benzoate[1] and methyl *p*-bromobenzoate[1], respectively, in the procedure described for *o*-nitrobenzhydrazide.

The hydrazine, acetic acid, salicylaldehyde, and solvents used and the syntheses of acethydrazide and diacetylhydrazine were described previously (7).

Synthesis of N-*Acetyl*-N′-m-*nitrobenzoylhydrazine* (*V*)—A mixture of 2.78 g of IV (0.015 mole) and 15 ml of acetic anhydride (0.18 mole) was refluxed for 2 hr. Then 15 ml of pyridine was added, and the reflux was continued for 4 more hr. The solution was evaporated under reduced pressure, and the remaining solid was dissolved in alcohol. The solution was kept in a refrigerator overnight, and brownish-yellow crystals precipitated. Light-yellow crystals (mp 192°), dried overnight *in vacuo*, were obtained by recrystallization from alcohol and then methanol.

The purity of V was corroborated by both TLC (100-μm silica, 7.5% isopropanol in chloroform, R_f 0.62) and HPLC (described later).

Synthesis of N,N′-*Bis*(m-*nitrobenzoyl*)*hydrazine* (*VI*)—To a 100-ml low actinic volumetric flask containing 50 ml of acetic acid, 5.45 g (0.03 mole) of IV was transferred. After the solid had dissolved, the flask was stoppered, the stopper closure was covered with aluminum foil, and the flask was left at room temperature in a closed cabinet. A flaky precipitate appeared on the 2nd day, and the quantity increased rapidly with time. After 10 days, the white precipitate was filtered off and recrystallized twice from hot acetic acid. After drying for 48 hr *in vacuo*, the dried crystals had a melting point of 242.2° [lit. (2) mp 242.0°].

The purity of VI was checked by HPLC (described later).

Acetous perchloric acid, about 0.1 *N*, was prepared according to Fritz (8).

α-Naphtholbenzein indicator solution was prepared by dissolving about 0.1000 g of the dye in enough acetic acid to make 100 ml.

Salicylaldehyde Reagent Solution—Exactly 50 ml of salicylaldehyde[1] was diluted to 100 ml with isopropanol.

Standard solutions for I, II, and IV–VI were prepared at concentration levels such as those encountered in the analysis for the respective compound, using the chromatographic mobile phase as the solution solvent. Except for I and II, all other solutions were used directly. Standard Solutions I and II were diluted as necessary and subjected to salicylaldehyde derivatization concomitantly with the kinetic samples undergoing analysis for I–III.

HPLC Mobile Phases and Columns—All mobile phases were filtered and degassed prior to use. The normal phase system for measurement of IV–VI consisted of 7.5% (v/v) isopropanol in chloroform and a 100-cm × 2-mm i.d. stainless steel tube packed manually with a pellicular silica gel[3] adsorbent.

The reversed-phase system for measurement of I–III consisted of 47% (v/v) acetonitrile in 0.14 *M* aqueous potassium dihydrogen phosphate and a 30-cm × 4-mm i.d. stainless steel tube packed with spherical siliceous microbeads, 5–10 μm, chemically bonded to a monomolecular layer of octadecyltrichlorosilane[4].

Instrumentation—The potentiometric titrations were carried out using the electrode system and the automatic potentiometric titrator (as used for IV) described by Medwick and Kirschner (9).

The modular HPLC instrument was described previously (7). All mobile phases were pumped at a flow rate of 1 ml/min.

Solutions were kept at a desired constant temperature in a water bath whose temperature was thermostatically controlled[5] to ±0.01° of the nominal setting.

Procedures—Throughout the described procedures, low actinic glass volumetric flasks and erlenmeyer flasks were used. For HPLC analysis, the appropriate standard solutions were run concomitantly with sample solutions.

Kinetic Studies—All kinetic runs were conducted in duplicate.

Solution Preparation and Sampling Acetous solutions (usually 0.06 *M*) of the hydrazine derivative were prepared by weighing accurately an appropriate quantity and dissolving it in and bringing to volume with acetic acid. The solution, usually kept at the temperature of the kinetic study in a water bath, was sampled at desired times, and the aliquots were transferred to suitable glassware for the analytical procedure.

For indicator titration or potentiometric titration, two 10.00-ml aliquots in separate 250-ml beakers were used. For the HPLC normal phase system (IV–VI analysis), two 2.00-ml aliquots in separate 10-ml volumetric flasks were used. For the HPLC reversed-phase system (I–III analysis), four 2.00-ml aliquots in separate 10-ml volumetric flasks were

[1] Eastman White Label.
[2] Matheson, Coleman and Bell.
[3] HC Pellosil, Whatman, Inc., Clifton, N.J.
[4] μBondapak C_{18}, Waters Associates, Milford, Mass.
[5] Lauda/Brinkmann circulator model K-2/RD.

Table I—Degradative Behavior of Some Aryl-, Carbamyl-, and Aroylhydrazines

Compound	Apparent First-Order Rate Constant, $sec^{-1} \times 10^6$
Arylhydrazines	
Phenylhydrazine	3.65
p-Bromophenylhydrazine	8.75
Carbamylhydrazines	
Semicarbazide	8.75
4-Phenylsemicarbazide	4.46
4-Phenyl-3-thiosemicarbazide	2.97
Aroylhydrazines (hydrazides)	
Benzhydrazide	2.01
o-Nitrobenzhydrazide	2.11
m-Nitrobenzhydrazide	1.67
p-Nitrobenzhydrazide	1.51
p-Bromobenzhydrazide	1.87

used. The aliquots were kept at 0.0° until sample collection for a particular run was completed and analyses were to be performed.

In the study of acetic acid dependence, six different 0.06 *M* IV solutions were prepared in solutions of varying pure acetic acid concentration in chloroform: 8.74, 5.25, 3.5, 1.75, and 0.874 *M*. The procedure was as described for the general case.

For analysis by indicator titration or potentiometric titration, the beakers were removed from the freezer, and 75 ml of acetic acid was added. The aliquots were titrated using α-naphtholbenzein indicator or according to the potentiometric titration procedure described by Medwick and Kirschner (9).

For HPLC analysis of IV–VI, the normal phase system was used for measurement. After the aliquots were removed from the freezer and brought to volume with the corresponding mobile phase, the solutions were analyzed by HPLC. Calculations were performed using:

$$W_u = \frac{H_u}{H_s} W_s p \qquad \text{(Eq. 1)}$$

where W_u is the weight, in grams, of the specified component in the sample solution; H_u is the peak height of the specified component in the sample chromatogram; H_s is the peak height of the specified component in the standard chromatogram; W_s is the weight, in grams, of the corresponding standard; and p is the purity of the standard, expressed as a decimal.

For HPLC analysis of I–III, the reversed-phase system was used for measurement. After the aliquots were removed from the freezer, 1.00 ml of isopropanol was added to each flask. The solutions were divided into two equal parts. The first half was used for measuring the amount of I and II in solution as follows. To each flask, 0.05 ml of the salicylaldehyde reagent was added (calculated to be an approximate 50% stoichiometric excess), and the flasks were then transferred to a 55° water bath for 5 min to ensure complete derivatization. The flasks were then removed, and 4.00 ml of chloroform was added to each. Finally, all solutions were brought to volume with methanol and analyzed.

The second half of the solution was used for the determination of III in solution as follows. To each flask, 2.00 ml of aqueous alcoholic hydrochloric acid was added, and the flasks were then immersed in a 60° water bath for 5 min. The flasks were then removed, and 0.05 ml of the salicylaldehyde reagent was added to each. The flasks were treated afterward in the same manner as for I and II analysis. The quantity of III in solution was calculated as the difference between the total amount of I after hydrolysis and the amount of I and II obtained from a nonhydrolyzed sample.

RESULTS AND DISCUSSION

Kinetic Studies—Because of its accuracy and simplicity, potentiometric titration was used to determine the apparent overall pseudo-first-order rate constants (Table I) for the reactions of several hydrazine derivatives with acetic acid. These data establish the nature of the reaction and show, as expected, that hydrazides are generally more stable than other hydrazines, probably due to their weak basicity. Within hydrazides as a separate group, stability increased as the acidity of the parent acid increased, so *p*-bromobenzhydrazide (pKa 3.97) had a faster rate of degradation than *p*-nitrobenzhydrazide (pKa 3.42).

Since the potentiometric analysis cannot identify or measure the different degradation products, TLC was explored. A partially degraded solution of IV was spotted on a TLC plate (100-μm silica) with 7.5% isopropanol in chloroform as a mobile phase. The following compounds were identified after spraying with Ehrlich's reagent: I (R_f 0.05), II (R_f 0.40), V (R_f 0.62), VI (R_f 0.65), and IV (R_f 0.50). After spraying the plate with aqueous alcoholic hydrochloric acid, another spot was identified as III (R_f 0.58). Attempts to use TLC quantitatively were unsuccessful because of the incomplete resolution of the spots and the rapid volatilization of hydrazine from the plate.

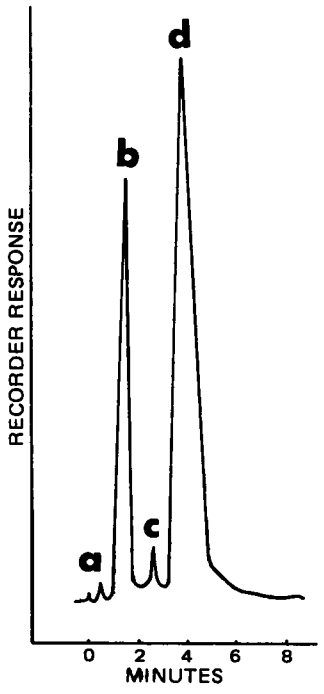

Figure 1—*HPLC analysis of* m-*nitrobenzhydrazide (IV) acetous solution at room temperature (after 6 hr) on pellicular silica with 7.5% isopropanol in chloroform as the mobile phase. Key: a, solvent; b,* N,N′-*bis*(m-*nitrobenzoyl)hydrazine (VI); c,* N-*acetyl*-N′-m-*nitrobenzoylhydrazine (V); and d,* m-*nitrobenzhydrazide (IV).*

HPLC was used successfully to quantitiate every component in solution. An HPLC system in the normal phase was developed to quantitate IV–VI. Figure 1 is a typical chromatogram. The chromatographic response for every compound was linear with a linear regression correlation coefficient of 0.999. The minimum limits of detectability were 6.1×10^{-5} *M* for VI, 1.79×10^{-4} *M* for V, and 2.8×10^{-4} *M* for IV. This system, however, can neither detect nor quantitate I–III because these compounds do not absorb UV radiation, as is required by the 254-nm detector. A refractive index detector was also inadequate for the trace analysis required in this study.

For these reasons, another system was developed whereby the salicylaldehyde derivatives of I and II (and of III after hydrolysis) were formed and separated on an HPLC reversed-phase column. The salicylaldehyde derivative of IV plus V and VI (both do not react with salicylaldehyde) also was resolved completely from the I and II derivatives, but the behavior of IV–VI did not allow their determination with this HPLC system. Figure 2 is a chromatogram showing the separation achieved using the reversed-phase system. The chromatographic response for both I and II was linear with concentration since both responses gave linear regression correlation coefficients of 0.9999; the minimum detectable quantities for I and II were 5×10^{-5} and 4.85×10^{-4} *M*, respectively.

Table II shows the temperature dependence of the IV reaction with acetic acid using HPLC analysis. HPLC analysis is specific in measuring a single compound whereas potentiometric analysis measures the total basicity of the solution; *i.e.*, any basic degradation product such as I or II would be titrated along with IV, so values of the rate constants would be inaccurate.

Table III describes the role of acetic acid concentration in the degradation of IV in acetous solution. Although the degradation reaction overall kinetics in excess acetic acid were pseudo-first order with respect to IV, the rate increased with the increase in the acetic acid concentration. An expression involving dependence on the acetic acid concentration may be written as:

$$\text{rate} = k'[\text{IV}] = k[\text{IV}][\text{HOAc}]^n \qquad \text{(Eq. 2)}$$

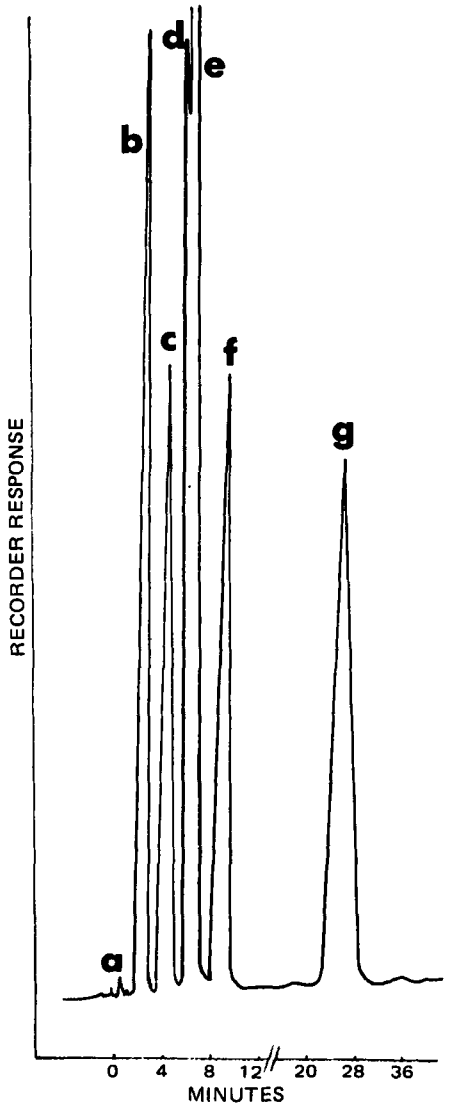

Figure 2—*Chromatogram of a synthetic mixture of the compounds to be found in a degraded acetous solution of* m-*nitrobenzhydrazide after derivatization with salicylaldehyde and using a reversed-phase column and acetonitrile (47%)-0.14 M potassium dihydrogen phosphate (53%) as the mobile phase. Key: a, solvent; b,* N-*acetyl-*N′-m-*nitrobenzoylhydrazine (V); c, salicylaldehyde acethydrazone; d,* N,N′-*bis*(m-*nitrobenzoyl)hydrazine (VI); e, salicylaldehyde (excess); f, salicylaldehyde* m-*nitrobenzhydrazone; and g, salicylaldazine.*

It is noticed that $k' = k[\text{HOAc}]^n$. Taking the logarithm results in:

$$\log k' = \log k + n \log [\text{HOAc}] \qquad \text{(Eq. 3)}$$

where k' = pseudo-first-order rate constant, k = true bimolecular rate constant, and n = relative order with respect to acetic acid.

When log k' was plotted *versus* log [HOAc], the linear least-squares parameters calculated were correlation coefficient 0.995 and intercept of 1.74×10^{-7} sec^{-1} (after taking the antilog). The calculated bimolecular rate constant was 2.90×10^{-6} liter mole^{-1} sec^{-1}. The slope value of n, the order relative to acetic acid, was calculated to be 0.82 by HPLC and 1.3 by potentiometric titration analysis; both values were close to first order.

The HPLC determination of the appearance and/or disappearance rates of the IV degradation products in acetic acid was conducted at 61°. This temperature was chosen since the I and II reaction with salicylaldehyde is very rapid at 60°. Thus, no temperature disturbance is introduced during analytical manipulations.

The reaction profiles of IV, I, V, and III are presented in Fig. 3. Although VI appeared almost instantaneously in acetous solutions of IV and increased regularly with time, it started to precipitate after about 3 hr due to its insolubility in acetic acid. Therefore, no accurate plot could be constructed for its appearance rate. Compound II, on the other hand, was not detected at any time in solution, even though the lower limit for its detection by the HPLC system was 4.85×10^{-4} *M*. As shown in Fig. 3, the IV concentration decreased regularly whereas I decreased after an initial increase. Both V and III increased monotonically with time.

Table II—Temperature Dependence of Degradation of IV in Acetic Acid Using HPLC Analysis

Temperature	First Order[a], $k \times 10^6$ sec^{-1}	E_a[b], kcal/mole
25.0°	2.06 (0.99)	
32.0°	3.39 (0.98)	14.7
42.2°	8.93 (0.999)	
61.0°	38.63 (0.999)	

[a] Values represent the rate constant and, in parentheses, the linear regression correlation coefficient. [b] For this Arrhenius plot, the linear least-squares parameters are: correlation coefficient, 0.999; slope, −3200 degree sec^{-1}; and intercept, +3.93 sec^{-1}.

The shape of the concentration profile of III in Fig. 3 is a consequence of the complicated reaction sequence, as will be seen later, in that III is formed in Schemes III, VII, and VIII but Scheme VIII gives rise to I, which subsequently appears as III. The same shape curve was observed in the study of the reaction of I and II with acetic acid (7).

The mechanism to be proposed for the reactions of IV with acetic acid must account for the presence of each degradation product and explain its concentration profile.

Although VI was reported (2) to form as an oxidation product of IV, an oxidation mechanism was disregarded in the present study because the degradation rate of the hydrazine derivative did not differ significantly when its acetous solution was kept in a nitrogen atmosphere in sealed ampuls or in air. Sealed ampuls filled with an acetous solution of IV under reduced pressure were analyzed by GC for any released nitrogen gas (as an oxidation by-product); no excess nitrogen gas was found, again indicating that no oxidation was operative. Photocatalyzed degradation was also eliminated because the degradation study was conducted in the dark and with solutions in low actinic glassware. The dependence of degradation on the acetic acid concentration suggested a mechanism in which acetic acid plays an active role.

Proposed Mechanism—After fitting different mechanisms to the experimental data, one scheme was arrived at as the most plausible mechanism consistent with the findings in the present study.

In the proposed mechanism (Schemes I–VIII), eight elementary reactions occur in the reaction of IV with acetic acid:

$$\text{IV} + \text{HOAc} \xrightarrow{k_0} \text{IV}^*$$
Scheme I

$$\text{IV}^* \xrightarrow{k_1} \text{V} + \text{H}_2\text{O}$$
Scheme II

$$2\,\text{IV}^* \xrightarrow{k_2} \text{VI} + \text{III}$$
Scheme III

$$\text{IV} + \text{IV}^* \xrightarrow{k_3} \text{VI} + \text{II}$$
Scheme IV

$$2\,\text{IV} \xrightarrow{k_4} \text{VI} + \text{I}$$
Scheme V

$$\text{I} + \text{HOAc} \xrightarrow{k_5} \text{II} + \text{H}_2\text{O}$$
Scheme VI

$$\text{II} + \text{HOAc} \xrightarrow{k_6} \text{III} + \text{H}_2\text{O}$$
Scheme VII

$$2\,\text{II} \xrightarrow{k_7} \text{III} + \text{I}$$
Scheme VIII

(k_5 + HOAc)

In this sequence, IV* is an intermediate and acetic acid is present in large excess.

Rate equations consistent with the elementary equations and that reflect overall system stoichiometry are:

$$\frac{d\text{IV}}{dt} = -k_0[\text{IV}] - k_3[\text{IV}][\text{IV}^*] - 2k_4[\text{IV}]^2 \qquad \text{(Eq. 4)}$$

$$\frac{d\text{IV}^*}{dt} = k_0[\text{IV}] - k_1[\text{IV}^*] - k_2[\text{IV}^*]^2 - k_3[\text{IV}][\text{IV}^*] \qquad \text{(Eq. 5)}$$

$$\frac{dV}{dt} = k_1[IV^*] \quad \text{(Eq. 6)}$$

$$\frac{dVI}{dt} = \tfrac{1}{2}k_2[IV^*]^2 + k_3[IV][IV^*] + k_4[IV]^2 \quad \text{(Eq. 7)}$$

$$\frac{dIII}{dt} = \tfrac{1}{2}k_2[IV^*]^2 + 2k_6[II] + k_7[II]^2 \quad \text{(Eq. 8)}$$

$$\frac{dII}{dt} = k_3[IV][IV^*] + 2k_5[I] - 2k_6[II] - 2k_7[II]^2 \quad \text{(Eq. 9)}$$

$$\frac{dI}{dt} = k_4[IV]^2 - 2k_5[I] + k_7[II]^2 \quad \text{(Eq. 10)}$$

The solution of this complex reaction pattern is presented in the *Appendix*. Table IV lists calculated rate constants. The reactions using actual structures are presented in Scheme IX.

The k_4 reaction was included to explain the rapid appearance of I in solution, which could not be accounted for by the k_7 reaction alone.

The reason for suggesting an intermediate or a transition state as an alternative route for the formation of VI was dictated by the fact that the rapid appearance rate of III and its high concentration were too large to be coming only from I in an indirect manner. Compound III had to be formed directly. Another possible route was the reaction of 2 moles of V to give VI plus III; however, this possibility was eliminated when V was found to be stable in acetic acid and no significant amount of VI formed in acetous solutions of V. The k_3 reaction in the mechanism was found necessary for the quantities of VI calculated to be present.

The nature of the intermediate has to be related to both IV and acetic acid, and its intrinsic structure has to have the ability of yielding either V or VI and III very rapidly. To understand the chemical nature of the intermediate, experiments were carried out in which solutes were introduced to disturb the acetic acid autoprotolysis to observe the effect, if any, on the reaction kinetics.

Table III—Dependence of IV Degradation on Acetic Acid Concentration at 25.0° by HPLC Analysis

Acetic Acid in Chloroform, *N*	Pseudo-First Order[a], $k \times 10^7$ sec^{-1}
17.4 (pure acetic acid)	20.60 (0.99)
8.740	9.61 (0.99)
5.250	5.90 (0.998)
3.500	4.72 (0.98)
1.750	2.83 (0.97)
0.874	1.63 (0.99)

[a] Values represent the rate constant and, in parentheses, the linear regression correlation coefficient.

Sodium acetate, triphenylguanidine, strong bases, and benzoic acid, a weak acid, had no significant effect on the reaction rate of IV with acetic acid. Perchloric acid, a strong acid, decreased the rate sharply, depending on its concentration. This finding may be explained if it is recognized that perchloric acid ties up an equivalent amount of IV in the protonated form and thus decreases the effective concentration of unprotonated IV available for the degradation reaction with acetic acid.

Although the details of the kinetic calculations are given in the *Appendix*, the agreement between the experimental data and the proposed mechanism should be discussed, particularly in light of the approximations used to solve this complex system. If $k = 38.63 \times 10^{-6}$ at 61.0° is used from Table II together with the experimental value for [IV] of 0.0315 at 5 hr (Fig. 3), the time chosen for the calculations, the experimental value for the disappearance of IV may be calculated using:

$$\frac{dIV}{dt} = -k[IV] = 12.2 \times 10^{-7} \text{ mole sec}^{-1} \quad \text{(Eq. 11)}$$

Equation 4 reduces to first-order form since $-2k_4[IV]^2$ is small when

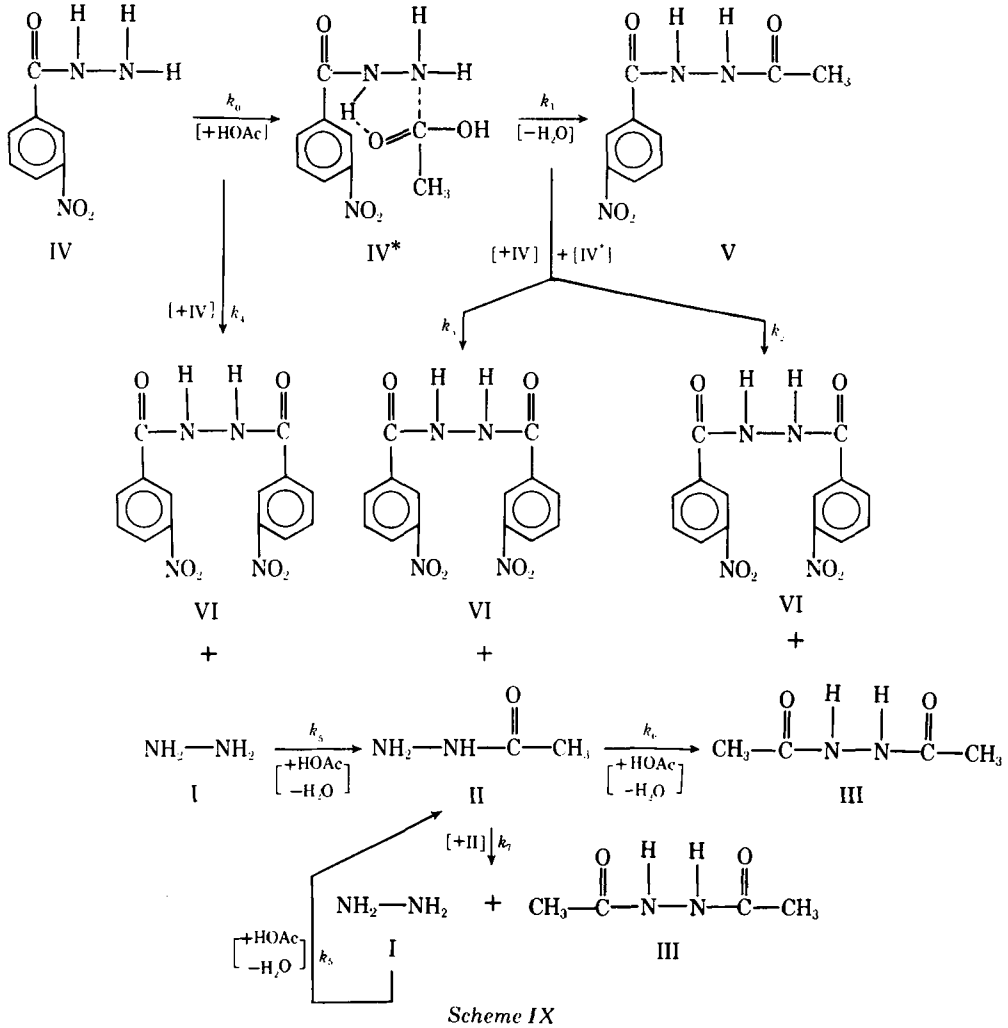

Scheme IX

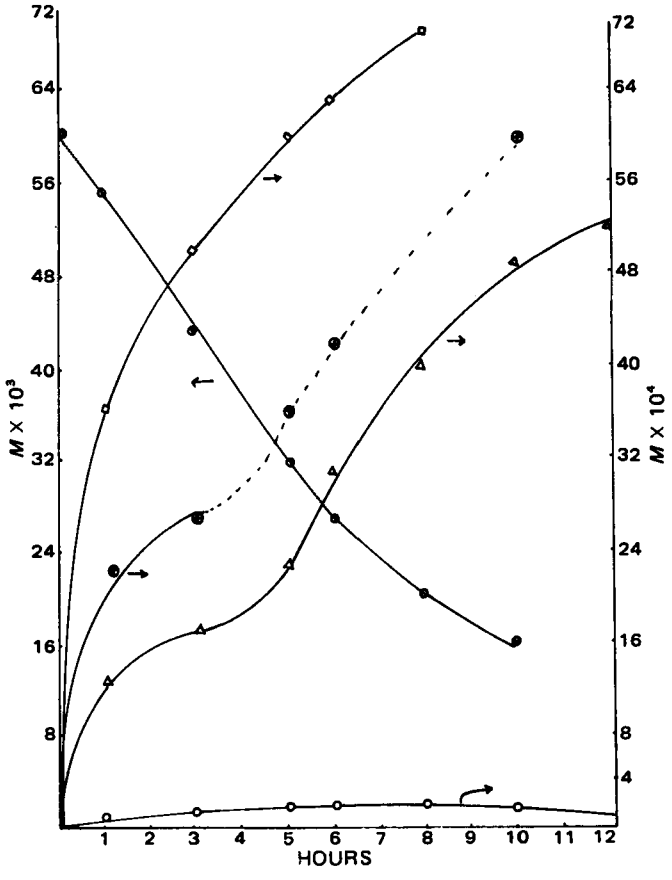

Figure 3—*Concentration profiles of* m-*nitrobenzhydrazide and its degradation products in acetic acid solution at 61°. Key:* ○, *I*, M × 10^{-4}; △, *III*, M × 10^{-4}; □, *V*, M × 10^{-4}; ⊘, *IV*, M × 10^{-3}; *and* ⊕, *VI*, M × 10^{-4}. *Compound VI precipitated from solution after 3 hr.*

the k values from Table IV, the linear least-squares line concentration at 5 hr from Fig. 3 for [IV] of 0.0345, and the [IV*] value of 2.52×10^{-3} M from Table V are used as in:

$$\frac{d\text{IV}}{dt} = -7.176 \times 10^{-7} - 3.558 \times 10^{-7} - 1.42 \times 10^{-7}$$

$$\cong -10.732 \times 10^{-7} \text{ mole sec}^{-1} \qquad \text{(Eq. 12)}$$

The value of $-2k_4[\text{IV}]^2$ constitutes only 13% of the total value of $d\text{IV}/dt$. Thus, since [IV*] is invariant owing to its steady state, the approximate form of Eq. 4 as a first-order rate equation may be written as:

$$\frac{d\text{IV}}{dt} = -[\text{IV}](k_0 + k_3[\text{IV}^*]) \qquad \text{(Eq. 13)}$$

When the least-squares value for [IV] from Fig. 3, the k_0 and k_3 values from Table IV, and the [IV*] value from Table V are substituted into Eq. 13, the result is 10.73×10^{-7} mole sec^{-1}. This calculated result agrees with the experimental value of Eq. 11 within 12%.

Another test of the agreement between predicted values and experimental data may be carried out for V. Equation 14 may be evaluated using $k_1 = 4.64 \times 10^{-5}$ sec^{-1} from Table IV and [IV*] = 2.52×10^{-3} M from Table V:

$$\frac{d\text{V}}{dt} = k_1[\text{IV}^*] = 1.17 \times 10^{-7} \text{ mole sec}^{-1} \qquad \text{(Eq. 14)}$$

If the experimental concentrations for [V] are plotted *versus* time in a first-order fashion, a straight line results (correlation coefficient = 0.987, excluding the first point) and gives a first-order rate constant of 1.60×10^{-5} sec^{-1}. When this rate constant is used with the experimental value for [V] at 5 hr, the point chosen for use in the approximation, Eq. 15 results:

$$\frac{d\text{V}}{dt} = k''[\text{V}] = 0.954 \times 10^{-7} \text{ mole sec}^{-1} \qquad \text{(Eq. 15)}$$

The predicted rate of Eq. 14 is within 18% of the experimental rate seen in Eq. 15. This good agreement adds credence to the approximations used to interpret the observed kinetics. The k'' (Eq. 15) is not the same as k_1 since the appearance rate of [V] is actually a function of the processes described in Schemes I and II.

Table IV—Rate Constants Calculated for Reactions Occurring in Acetous Solution of IV at 61°

Rate Constant	Value
k_0	2.08×10^{-5} sec^{-1}
k_1	4.64×10^{-5} sec^{-1}
k_2	3.90×10^{-2} liter mole^{-1} sec^{-1}
k_3	4.09×10^{-3} liter mole^{-1} sec^{-1}
k_4	5.89×10^{-5} liter mole^{-1} sec^{-1}
k_5	2.09×10^{-5} sec^{-1}
k_6	8.89×10^{-6} sec^{-1}
k_7	2.03×10^{-3} liter mole^{-1} sec^{-1}

Another convenient index of the rationality of a proposed mechanism is the calculated mass balance and its agreement with experimental values. Attempts to establish the mass balance relationship in this case were hampered by the insolubility of VI and the fact that II was beyond the limit of detection. With these limitations, calculation accounted for about 80% of the initial concentration of IV. This amount is reasonable and expected.

APPENDIX

The following symbols will be used: I, hydrazine; II, acetylhydrazine; III, diacetylhydrazine; IV, *m*-nitrobenzhydrazide; V, *N*-acetyl-*N'*-*m*-nitrobenzoylhydrazine; and VI, *N,N'*-bis(*m*-nitrobenzoyl)hydrazine.

The rate constants specified in Schemes I–VIII and found in the differential equations (Eqs. 4–10) that describe the reaction rates of the six hydrazine compounds in the IV–acetic acid system were evaluated.

Preliminary Considerations—Before the solution is described, several assumptions should be considered.

1. Due to the presence of both consecutive and parallel bimolecular reactions in the suggested mechanism, difficulties were encountered in integrating the differential rate equations. Mathematical treatments reported by Chien (10) and by Pearson *et al.* (11) for less complicated mechanisms, which involved either consecutive or parallel bimolecular reactions using transforms and introduction of Bessel functions, were investigated; however, the solution was complicated in this case because of the presence of the hydrazine loop (Scheme VIII, k_7, and Scheme VI, k_5). Although an exact solution for this complicated mechanism may be possible, an approximation was used.

Since the concentration–time profiles for each compound over the timespan studied (Fig. 3) are obviously not linear, some points were neglected to obtain linear least-squares lines for each profile. To indicate the nature of the lines, the points neglected are mentioned, together with the linear correlation coefficient of the resulting straight line: IV, all points used, 0.984; V, first point neglected, 0.993; I, first point neglected, 0.999; and III, last two points neglected, 0.983. This approach permitted use of slopes for derivatives, *e.g.*, $d\text{IV}/dt = \Delta\text{IV}/\Delta t$.

When the concentration of a reactant or product was required, the value on the least-squares line at 5 hr, approximately the midpoint representing a point where deviation of the least-squares point from experimental values would be the least, was chosen in solving the rate equations. In some cases, these solutions were compared with the solution obtained using actual experimental concentrations at 5 hr.

2. In a separate study of I and II reactions with acetic acid at 61° (7), k_5, k_6, and k_7 were determined. The average value for each rate constant was: k_5, 7.53×10^{-2} hr^{-1}; k_6, 3.20×10^{-2} hr^{-1}; and k_7, 7.32 liters mole^{-1} hr^{-1}.

3. Because II was not detected in solution during the study (lower limit of detectability was 4.8×10^{-4} M), its concentration was considered small enough so that when it or its square was multiplied by k_6 or k_7, respectively, the [II] and $[\text{II}]^2$ terms in Eqs. 8 and 10 were negligible and Eqs. A1 and A2, respectively, resulted:

$$\frac{d\text{III}}{dt} = \tfrac{1}{2}k_2[\text{IV}^*]^2 \qquad \text{(Eq. A1)}$$

$$\frac{d\text{I}}{dt} = k_4[\text{IV}]^2 - 2k_5[\text{I}] \qquad \text{(Eq. A2)}$$

Equation A1 is valid after about 3.5 hr. Prior to this point, the disproportionation of II and the production of I cause the unusual saddle region seen in the profile for III in Fig. 3.

4. A steady-state approximation can be used for Eq. 5, *i.e.*, $\Delta\text{IV}^*/\Delta t$

Table V—Calculated Values for k_3, k_2, k_1, and [IV*]

Reaction Variable	Set 1	Set 2
k_3, liters mole^{-1} hr^{-1}	14.74	7.66
k_2, liters mole^{-1} hr^{-1}	140.4	37.91
k_1, hr^{-1}	1.67×10^{-1}	8.67×10^{-2}
[IV*], M	2.52×10^{-3}	4.9×10^{-3}

= 0. This assumption was supported by the fact that k_0 can be considered significantly smaller than both k_2 and k_3, as was proven to be true in both I and II studies (7). This condition allows very small changes in [IV*] during the short period between its formation and degeneration to the final products. If the steady-state approximation is used, Eq. 5 may be written as:

$$k_0[\text{IV}] = k_1[\text{IV*}] + k_2[\text{IV*}]^2 + k_3[\text{IV}][\text{IV*}] \qquad \text{(Eq. A3)}$$

Calculation of Rate Constants—Substituting the experimental value of $\Delta\text{III}/\Delta t$ from Fig. 3 into Eq. A1 gives:

$$[\text{IV*}]^2 = 8.92 \times 10^{-4}\, k_2^{-1} \qquad \text{(Eq. A4)}$$

The experimental value for $\Delta V/\Delta t$ from Fig. 3 is substituted into Eq. 6 and yields Eq. A5:

$$\Delta V/\Delta t = k_1[\text{IV*}] = 4.324 \times 10^{-4}\, M\ \text{hr}^{-1} \qquad \text{(Eq. A5)}$$

Substitution of Eqs. A4 and A5 into Eq. A3 results in:

$$k_0[\text{IV}] = 0.0004324 + 0.000892 + k_3[\text{IV}][\text{IV*}] \qquad \text{(Eq. A6)}$$

Approximating $d\text{IV}/dt$ as $\Delta\text{IV}/\Delta t$ in Eq. 4 and adding this modified equation to Eq. A6 produces:

$$2k_0[\text{IV}] + (\Delta\text{IV}/\Delta t) = 0.0013244 - 2k_4[\text{IV}]^2 \qquad \text{(Eq. A7)}$$

From Fig. 3, values are introduced for $\Delta\text{I}/\Delta t$ and [I] into Eq. A2:

$$\Delta\text{I}/\Delta t = 0.000212 = k_4[\text{IV}]^2 - 2(0.0753)(0.00017) \qquad \text{(Eq. A8)}$$

$$k_4[\text{IV}]^2 = 0.000240 \qquad \text{(Eq. A9)}$$

Substitution of the Fig. 3 linear least-squares (at 5 hr) value of IV = 0.0345 M into Eq. A9 yields:

$$k_4 = 2.1 \times 10^{-1}\ \text{liter mole hr}^{-1} \qquad \text{(Eq. A10)}$$

Substitution for k_4 from Eq. A10 and for [IV] and $\Delta\text{IV}/\Delta t$ from Fig. 3 in Eq. A7 produces:

$$2k_0(0.0345) - 0.004364 = 0.0008245 \qquad \text{(Eq. A11)}$$

The value for k_0 is thus 7.51×10^{-2} hr^{-1}. Substitution of the values for k_0 and k_4 in Eq. 4, where $d\text{IV}/dt$ is approximated as $\Delta\text{IV}/\Delta t$, yields:

$$-0.004364 = -0.0751(0.0345) - k_3(0.0345)[\text{IV*}] - 2(0.212)(0.0345)^2 \qquad \text{(Eq. A12)}$$

$$[\text{IV*}] = 0.0371k_3^{-1} \qquad \text{(Eq. A13)}$$

If the values for [IV*] and [IV*]^2 are substituted into Eq. A3, Eq. A14 results:

$$(0.0751)(0.0345) = 0.0371k_1k_3^{-1} + (0.0345)(0.0371) + k_2(0.0371)^2k_3^{-2} \qquad \text{(Eq. A14)}$$

Multiplying Eq. A14 by k_3^2 and rearranging result in:

$$0.00131k_3^2 = 0.0371k_1k_3 + 0.00138k_2 \qquad \text{(Eq. A15)}$$

Equations A14 and A13 are equated to yield:

$$k_2 = 0.646k_3^2 \qquad \text{(Eq. A16)}$$

Substituting this value for k_2 into Eq. A15 yields:

$$0.00131k_3^2 = 0.0371k_1k_3 + 0.00138(0.646)k_3^2 \qquad \text{(Eq. A17)}$$

$$k_3 = 88.31k_1 \qquad \text{(Eq. A18)}$$

Substitution for k_3 from Eq. A18 into Eq. A16 results in:

$$k_2 = (88.31)^2k_1^2/1.547 \qquad \text{(Eq. A19)}$$

At this point, values for k_0, k_4, k_5, k_6, and k_7 are known. However, it is necessary to obtain values for k_1, k_2, and k_3 with Eqs. A4, A18, and A19 such that the range of values of [IV*] satisfies mass balance restrictions. The mass balance statement based on [IV] (initial) = 0.06 M is only approximate since [II] is small and below the limit of detectability and [VI] can be determined only approximately since it precipitates from solution.

The values at 5 hr of [IV], [V], [I], and [III] were obtainable from Fig. 3. The amount of [VI] that had precipitated was estimated by gravimetric analysis following simple filtration of a solution aliquot, and this value was added to the [VI] in solution at 5 hr. The approximate sum of all [IV]-derived species was 0.056, exclusive of [IV*]; thus, to satisfy the [IV] (initial) of 0.06 M, the [IV*] must be less than 0.004 M.

The solution of Eqs. A4, A18, and A19 for k_1, k_2, k_3, and [IV*], the latter still being unknown even though a range of values is known to be acceptable, is not possible by usual means since four unknowns cannot be calculated from three equations. Empirical trials were carried out to discover an additional relationship between [IV*] and the unknown constants. By assuming values for k_1, values for k_2, k_3, and [IV*] were computed using computer calculation. For [IV*] to be less than 0.004 M as required, it was found that k_1 had to be larger than 0.08.

A number of plots of [IV*] *versus* k_2 and k_3 in different forms showed that useful relationships exist when [IV*]^2 was plotted against k_3/k_2 or $1/k_3$. In both instances, a straight-line relationship was obtained (correlation coefficient of 0.993) in the valid range of k_1, *i.e.*, k_1 larger than 0.08. Equation A20 is written using the slope and intercept values from the linear plot of k_3/k_2 *versus* [IV*]^2:

$$k_3/k_2 = 0.0691 + 5643[\text{IV*}]^2 \qquad \text{(Eq. A20)}$$

Substituting for [IV*]^2 from Eq. A4 into Eq. A20 gives:

$$k_3 = 0.0691k_2 + 5.04 \qquad \text{(Eq. A21}a\text{)}$$

or:

$$k_2 = 14.47k_3 - 72.94 \qquad \text{(Eq. A21}b\text{)}$$

Equation A16 is used to substitute into Eqs. A21a and A21b, yielding a quadratic equation for k_3:

$$k_3 = \frac{14.47 \pm \sqrt{209.38 - 4(0.646)(72.94)}}{2(0.646)} \qquad \text{(Eq. A22)}$$

which may be solved to yield two values of k_3. The existence of two values for k_3 leads to pairs of values for k_2, k_1, and [IV*] (Table V). A decision between the acceptability of data of Sets 1 and 2 in Table V was based on the requirements of the mass balance of all species arising from [IV] (initial). If the values from Set 2 of [IV*] are included in the mass balance, then the total IV-derived species concentration is larger than the experimental [IV] (initial); however, use of [IV*] from Set 1 makes the total IV-derived species concentration agree well with the known experimental value for [IV] (initial), 0.06 M.

REFERENCES

(1) B. Camber, *Clin. Chim. Acta*, **2**, 188 (1957).

(2) H. Strain, *J. Am. Chem. Soc.*, **57**, 758 (1935).

(3) L. Stattler and F. W. Zerban, *ibid.*, **70**, 873 (1948).

(4) H. E. Malone, "The Determination of Hydrazino-Hydrazide Groups," Pergamon, New York, N.Y., 1970.

(5) M. L. Blake, D. Bode, and H. J. Rhodes, *J. Pharm. Sci.*, **63**, 1303 (1974).

(6) W. C. Harris and K. G. Stone, *J. Org. Chem.*, **23**, 2032 (1958).

(7) H. M. Abdou and T. Medwick, *J. Org. Chem.*, **43**, 15 (1978).

(8) J. S. Fritz, "Acid-Base Titrations in Nonaqueous Solvents," G. Frederick Smith Chemical Co., Columbus, Ohio, 1952, p. 13.

(9) T. Medwick and E. Kirschner, *J. Pharm. Sci.*, **55**, 1296 (1966).

(10) J. Chien, *J. Am. Chem. Soc.*, **70**, 2256 (1948).

(11) R. G. Pearson, L. C. King, and S. H. Langer, *J. Am. Chem. Soc.*, **73**, 4149 (1951).

ACKNOWLEDGMENTS

Adapted in part from a thesis submitted by H. M. Abdou to the Graduate School, Rutgers University, in partial fulfillment of the Doctor of Philosophy degree requirements.

Thanks are extended to Dr. Takeru Higuchi, University of Kansas, for advice and encouragement and to the Wisconsin Alumni Research Foundation for aid. Gratitude is expressed to Dr. F. J. Cioffi and Mr. Robert Lanza, E. R. Squibb and Sons, for help with the calculations. Mr. Donald Martone is thanked for technical aid.